Oxygen Stable Electrochemical CO_2 Capture and Concentration through Alcohol Additives

Jeffrey M. Barlow[1], Jenny Y. Yang[1*]

[1]Department of Chemistry, University of California, Irvine; Irvine, CA 92697 USA
*Corresponding author. Email: j.yang@uci.edu

Abstract: Current methods for CO_2 capture and concentration (CCC) are energy intensive due to their reliance on thermal cycles, which are intrinsically Carnot limited in efficiency. In contrast, electrochemically driven CCC (eCCC) can operate at much higher theoretical efficiencies. However, most reported systems are sensitive to O_2, precluding their practical use. In order to achieve O_2 stable eCCC, we pursued the development of molecular redox carriers with reduction potentials positive of the O_2/O_2^- redox couple. Prior efforts to chemically modify redox carriers to operate at milder potentials resulted in a loss in CO_2 binding. To overcome these limitations, we used common alcohols additives to anodically shift the reduction potential of a quinone redox carrier, 2,3,5,6-tetrachloro-*p*-benzoquinone (TCQ), by up to 350 mV, conferring O_2 stability. Intermolecular hydrogen-bonding interactions to the dianion and CO_2-bound forms of TCQ were correlated to alcohol pK_a to identify ethanol as the optimal additive, as it imparts beneficial changes to both the reduction potential and CO_2 binding constant, the two key properties for eCCC redox carriers. We demonstrate a full cycle of eCCC in aerobic simulated flue gas using TCQ and ethanol, two commercially available compounds. Based on the system properties, an estimated minimum of 21 kJ/mol is required to concentrate CO_2 from 10% to 100%, or twice as efficient as state-of-the-art thermal amine capture systems and other reported redox carrier-based systems. Furthermore, this approach of using hydrogen-bond donor additives is general and can be used to tailor the redox properties of other quinones/alcohol combinations for specific CO_2 capture applications.

Avoiding the most severe climate effects from anthropogenic carbon dioxide (CO_2) emissions requires the advancement of CO_2 capture and concentration (CCC) technology. Currently, most approaches to CCC use thermal swings, which are energetically inefficient and expensive.[1] There are several advantages for using electrochemical methods (eCCC) over thermal-swings. These include independence from Carnot limitations to achieve theoretical efficiencies of up to 100%, operation at ambient temperatures, modular scalability for point source applications, and the use of increasingly economical renewable electricity.[2–4]

A common approach to eCCC is the use of redox carriers.[4–6] Redox carriers have two stable oxidation states, shown as **R** and $\mathbf{R^{n-}}$ in Scheme 1. In the reduced state ($\mathbf{R^{n-}}$), the carrier has a high binding constant ($K_{1,CO2}$) to facilitate CO_2 capture from dilute streams. In the oxidized state (**R**), the carrier has a low binding constant ($K_{2,CO2}$) allowing for CO_2 release and concentration. Several classes of redox-active carriers have been investigated for eCCC applications including bipyridines,[7–9] thiols,[10] and quinones.[11–18] However, eCCC systems generally degrade from aerobic input streams because the reduced carriers react with oxygen (O_2) resulting in unproductive

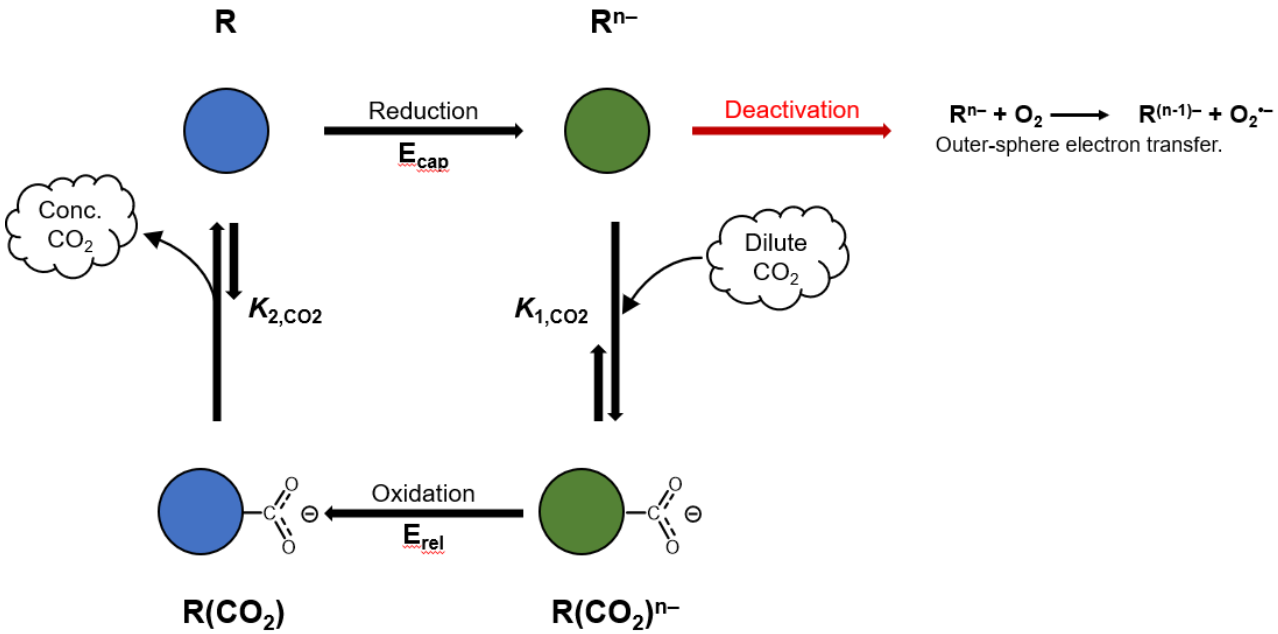

Scheme 1: General process for eCCC systems featuring a redox carrier in its resting state (**R**) that binds to CO_2 upon reduction (to $\mathbf{R^{n-}}$) to form $\mathbf{R(CO_2)^{n-}}$ with a CO_2 binding constant of $\boldsymbol{K_{1,CO2}}$. Upon oxidation of $\mathbf{R(CO_2)^{n-}}$ to form $\mathbf{R(CO_2)}$, CO_2 is released to regenerate the resting-state carrier, **R**. If O_2 is present, deactivation of the active carrier can occur through electron transfer.

carrier oxidation and the generation of superoxide, which can cause destructive radical reactions with the carrier, solvent, or electrolyte (red reaction in Scheme 1).[19,20] Since oxygen is present in flue gas and atmospheric CO_2 sources, practical eCCC methods must overcome this limitation.

Aerobic stability is possible if $E_{1/2}(\mathbf{R/\ R^{n-}})$ (E_{cap} in Scheme 1) is positive of the $O_2/O_2^{\bullet-}$ reduction potential. The range of this reduction potential in a few different solvents is demarcated by the dashed black lines in Figure 1 (experimental measurements are shown in Figure S1). The second key parameter for a redox carrier is its CO_2 binding constant ($K_{1,CO2}$), which must also be

optimized for the application. For example, in order to attain >90% capture efficiency (>90% of incoming CO_2 is captured by the solution in a single pass), log($K_{1,CO2}$) must be greater than ~3.2 and ~5.5 for capture from flue gas and atmospheric concentrations, respectively.[11,12,22] The minimum value of log($K_{1,CO2}$) needed for flue gas or atmospheric capture is also shown as the dashed green and blue lines, respectively in Figure 1. The shaded green and blue regions indicate the working regimes required for O_2 stable eCCC from flue gas or atmospheric resources.

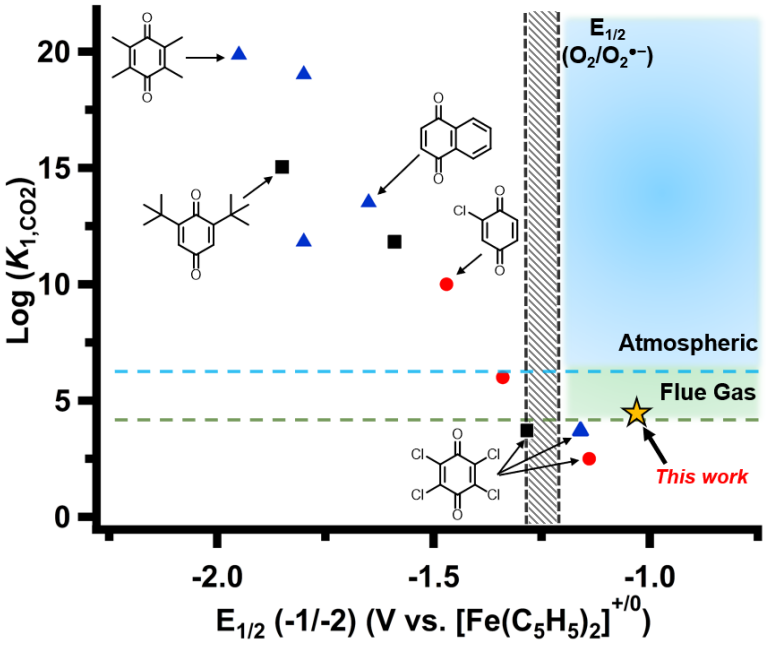

Figure 1. Relationship between reduction potential and CO_2 binding constant. Plot of Log($K_{1,CO2}$) versus $E_{1/2}$ for reported quinone dianion species in: DMF (black squares), DMSO (blue triangles), or CH_3CN (red circles), and TCQ in 2M EtOH in DMF as reported here (star). Selected structures are shown next to their corresponding data points. The vertical black dotted lines indicate the range of $O_2/O_2^{\bullet-}$ couples in the reported solvents. Dotted horizontal lines represent the minimum requirement of Log($K_{1,CO2}$) from flue gas (green) or atmospheric (blue) resources. Shaded regions display the working regimes necessary for flue gas (green) or atmospheric (blue) eCCC applications. Data for each quinone is listed in Table S1.

Among reported redox carriers for eCCC, quinones have shown particular promise, with greater CO_2 binding constants at milder potentials compared to other organic redox carriers (Figures 1 and S2).[4,7–10] Under anaerobic conditions, quinones have performed eCCC from concentrations of less than 1% to greater than 90%.[21,23] Quinones are also currently produced at large scales, economical, and easily modified through functionalization. Electronic structure modifications through functionalization of quinones results in a linear free energy relationship (LFER) between the binding constant (log($K_{1,CO2}$)) and reduction potential ($E_{1/2}$) (Figure 1). As a result, all previously explored redox carriers fall outside of the required working regimes for aerobic flue gas and atmospheric capture applications (Figure 1, Table S1).

As the two key properties for a redox carrier cannot be independently tuned through conventional functionalization, we pursued the use of intermolecular hydrogen bonding interactions through alcohol additives to break the LFER. Our studies demonstrate that common alcohol additives result in beneficial changes to the two key properties of a redox carrier – reduction potential and CO_2 binding constant. We also describe how hydrogen-bonding interactions are optimizable through the p*K*a of the alcohol additive. Using this approach, we demonstrate efficient O_2-stable eCCC from flue gas concentrations using a commercially available quinone and alcohol. [24–26]

The use of alcohol additives described herein provides a facile approach for tuning the redox carrier properties into desirable ranges that are not accessible through traditional molecular functionalization. This approach can be applied to optimize redox carrier properties for different eCCC applications using easily accessible quinone and alcohol combinations.

Results

Reduction of TCQ Under an N_2 Atmosphere and effect of added alcohols. Cyclic voltammetry (CV) of 2,3,5,6-tetrachloro-*p*-benzoquinone (TCQ) in the absence of hydrogen-bonding interaction under an N_2 atmosphere exhibits two reversible, one-electron reductions in polar aprotic solvents, such as dimethylformamide (DMF, black trace Figure 2A), dimethylsulfoxide, (DMSO, Figure S3), acetonitrile (CH_3CN), and benzonitrile (PhCN).[11–13,27] Similar to the studies reported by Linschitz and Gupta,[27] the addition of weakly acidic alcohols ($pK_a(H_2O) \geq 12.5$) to solutions of TCQ in DMF or DMSO under an N_2 atmosphere shifts the second reduction event ($E(TCQ^{\bullet-}/ TCQ^{2-})_{1/2}$) to more positive potentials, while the first reduction event ($TCQ/ TCQ^{\bullet-}$) remains unaffected (Figure 2a). Eight alcohol additives (2, 2, 2-trifluoroethanol (TFE), 2, 2, 2-tribromoethanol (TBE), ethylene glycol (EG), 2-methoxyethanol (2-ME), ethanol (EtOH), hexanol (HexOH), 2-propanol (i-PrOH), and *tert*-butanol (t-BuOH)) were used in this study and all resulted in anodic shifts in potential, with some in excess of 350 mV (Figure 2a). For all alcohols, the magnitude of the anodic shift increases with alcohol concentration; however, at each concentration the shift is larger for alcohols with lower pK_a values (Figure S4-S6, and Table S2 pK_a values are shown in Table 1). Both reduction events remain reversible with alcohol additives at all scan rates measured (ν = 10-1000 mV/sec, Figure S7 and Table S3). Cyclic voltammograms of chemically

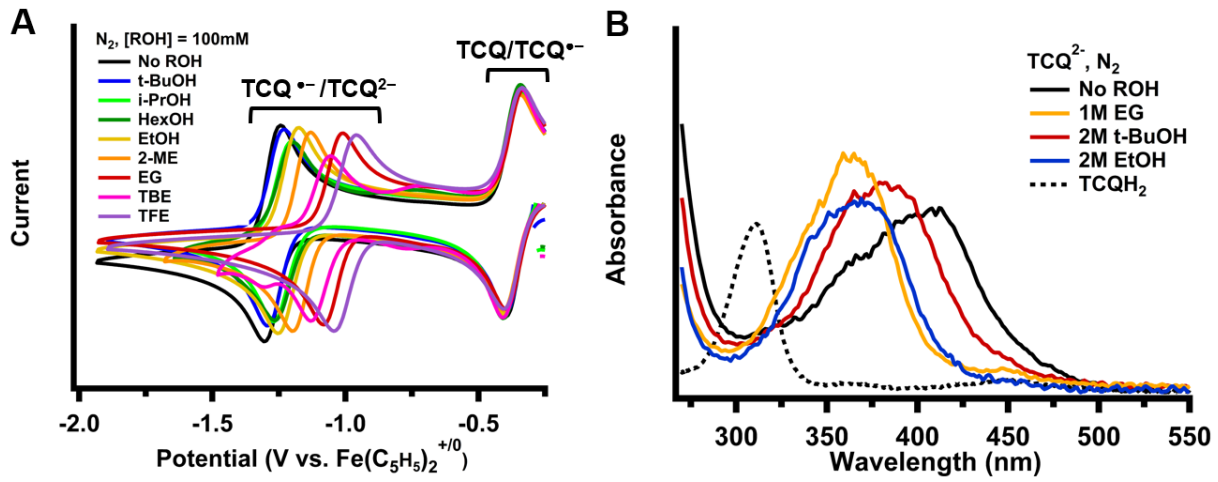

Figure 2. Effect of alcohol additives on reduction potential and electronic absorption spectra of TCQ. (a) Normalized cyclic voltammograms of TCQ containing 100mM concentrations of various alcohol additives; decreasing alcohol pK_a results in larger anodic shifts to the second redox event. All voltammograms were recorded using DMF solutions containing 0.2 M $TBAPF_6$ electrolyte and 2.0 mM TCQ analyte concentrations under N_2 atmosphere. (b) Normalized electronic absorption spectra of TCQ^{2-} obtained during UV-vis SEC experiments. Experiments were performed in DMF containing no alcohol (black trace), 1M ethylene glycol (orange trace), 2M ethanol (blue trace), or 2M tert-butanol (red trace) with 0.2 M $TBAPF_6$ electrolyte and 0.7 mM TCQ under N_2 atmosphere. For each solution, no protonation (to form the corresponding hydroquinone $TCQH_2$, (black dashed trace) is observed.

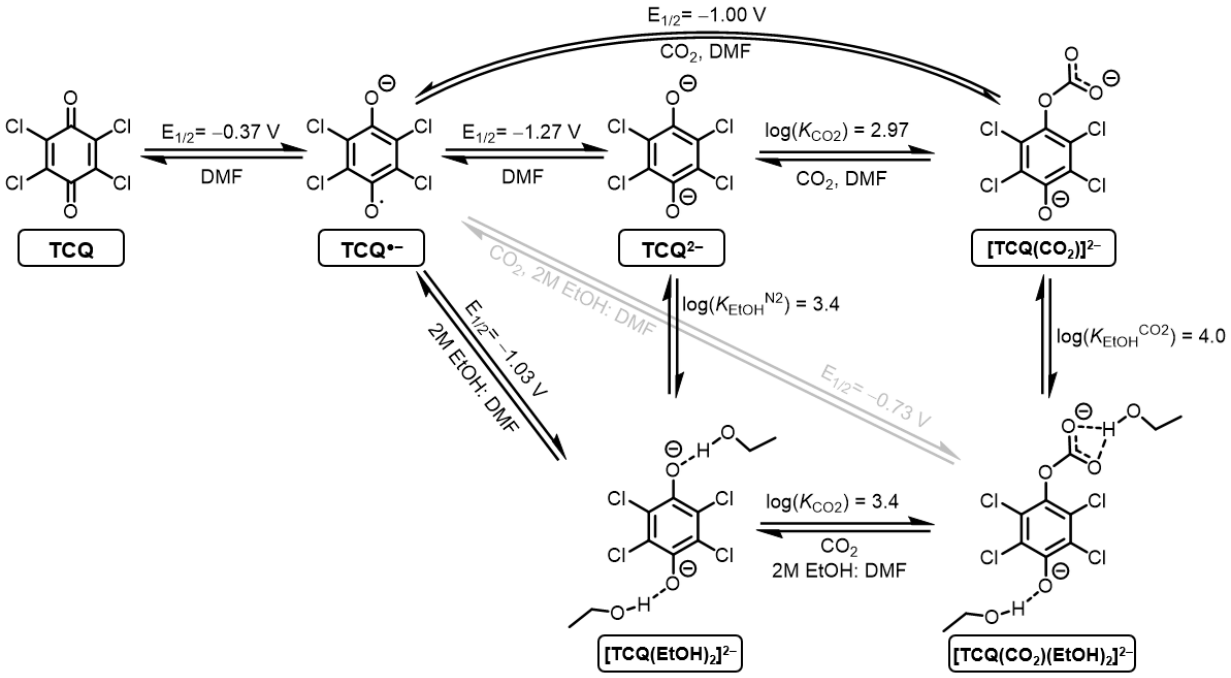

Scheme 2. $TCQ^{\bullet-}$ Properties in DMF and in 2M EtOH in DMF. Proposed reduction and CO_2 binding mechanism of TCQ with CO_2 in the presence and absence of intermolecular hydrogen-bonding interactions from ethanol. Experimentally determined thermodynamic values are shown for each step.

prepared $[TBA]_2[TCQ^{2-}]$ in DMF with 2M ethanol are nearly identical to that of TCQ in the same solvent mixture, with no evidence of decomposition after several hours (Figure S8).

Hydrogen-bonding interactions with EG, t-BuOH, and EtOH and the reduced TCQ species were further investigated using UV-visible spectroscopy and spectroelectrochemistry (UV-vis SEC). UV-vis SEC of TCQ in the absence of hydrogen-bond donors in DMF indicates that the quinone (TCQ), radical anion ($TCQ^{\bullet-}$), dianion (TCQ^{2-}), and doubly-protonated dianion ($TCQH_2$) have distinct absorbance features (Figure S9). The addition of alcohols results in a blue-shift (decrease in wavelength) in the absorbance of TCQ^{2-} (Figure 2b), while the absorbance spectra of TCQ, $TCQ^{\bullet-}$, and $TCQH_2$ are unaffected (Figure S10, S11). Further, this change in λ_{max} for TCQ^{2-} is larger for alcohols with lower pK_a (Figure 2b). However, while the shift in the absorption spectra of TCQ^{2-} indicates that the alcohols interact with the dianion, they do not correspond to $TCQH_2$, signifying TCQ^{2-} is not being protonated.[28] UV-visible spectra of chemically synthesized $[TBA]_2[TCQ^{2-}]$ has the same features and do not change over several hours (Figure S9). The spectroscopic, electrochemical, and spectroelectrochemical data all indicate that the alcohols hydrogen-bond to TCQ^{2-}, resulting in anodic shifts to the $E(TCQ^{\bullet-}/ TCQ^{2-})_{1/2}$ potential – in some cases positive of the $O_2/O_2^{\bullet-}$ reduction potential in DMF – without resulting in protonation or decomposition.

CO_2 Binding to TCQ Dianion and effect of alcohol additives.

Under an N_2 or CO_2 atmosphere, no changes occur in the UV-vis SEC absorption spectra of TCQ and singly reduced $TCQ^{\bullet-}$, confirming that neither species reacts with CO_2. In contrast the absorption spectra of TCQ^{2-} is significantly blue-shifted in the presence of CO_2 (dotted versus

solid traces, Figure S11), indicating CO_2 binding. Similar to other quinones, TCQ^{2-} reacts with CO_2 to form an aryl carbonate species (Scheme 2)[12,13], which we have characterized by ^{13}C NMR (Figure S13)[18] and Fourier-transform infrared (FTIR) spectroscopy (Figure S14).[15,18]

UV-vis SEC studies with added ethylene glycol, *tert*-butanol, and ethanol also result in no changes to the electronic absorption spectra between an N_2 and CO_2 atmosphere for TCQ and $TCQ^{\bullet-}$. However, the absorption corresponding to $[TCQ(CO_2)]^{2-}$ is further blue-shifted in the presence of alcohol additives (Figure 3b). Of the three alcohols, only ethylene glycol appears to protonate $TCQ^{2-}$to form $TCQH_2$, which was not observed under an N_2 atmosphere. The electronic absorption spectrum of chemically synthesized $[TBA]_2[TCQ^{2-}]$ in 2M ethanol in DMF under CO_2 is nearly identical to TCQ^{2-} generated electrochemically under the same conditions (Figure S15).

CO_2 binding at TCQ^{2-} is also evident by comparing the cyclic voltammograms of TCQ recorded under N_2 and CO_2 atmospheres. While the first reduction to $TCQ^{\bullet-}$ is identical under both conditions, the second reduction features an anodic shift in $E_{1/2}$ in the presence of CO_2, indicating an $E_rE_rC_r$ event, or two reversible electron transfer events followed by a rapid reversible chemical step (CO_2 binding, Figure 3a).[29,30] The addition of alcohol additives under CO_2 results in a further anodic shift in the second reduction event, $E(TCQ^{\bullet-}/ TCQ^{2-})_{1/2}$ (Figure 3a). The magnitude of the anodic shift correlates with increasing concentration and decreasing pK_a of the alcohol (Figures 3, S16, and S17). These results indicate that the alcohols also hydrogen-bond to the CO_2 adduct of TCQ^{2-} ($[TCQ(CO_2)]^{2-}$). Chemically synthesized $[TBA]_2[TCQ^{2-}]$ in the presence of ethanol under a CO_2 atmosphere feature CVs that are almost identical to solutions of TCQ under the same conditions, even after sitting in solution for several hours (Figure S18). CVs and electronic absorption spectra of a $[TBA]_2[TCQ(CO_2)^{2-}]$ solution after addition of ethanol are

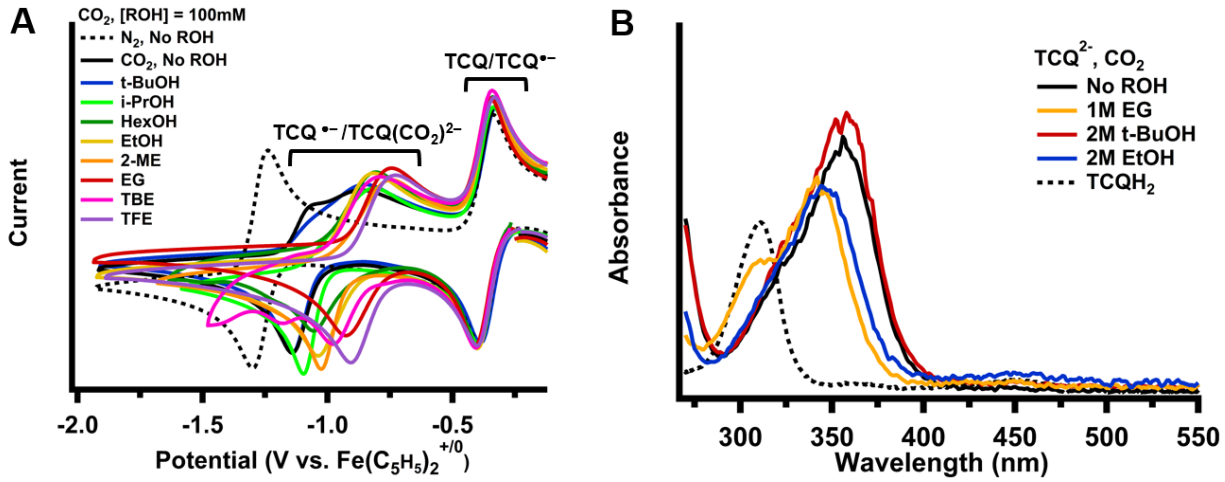

Figure 3. Effect of alcohol additives on the reduction potential and electronic absorption spectra of TCQ under 1 atm of CO_2. (a) Normalized cyclic voltammograms of TCQ under N_2, CO_2, and containing 100mM concentrations of various alcohol additives under CO_2; decreasing alcohol pK_a results in larger anodic shifts to the second redox event. All voltammograms were recorded in DMF solutions containing 0.2 M $TBAPF_6$ electrolyte and 2.0 mM TCQ analyte concentrations. (b) Normalized electronic absorption spectra of TCQ^{2-} obtained during UV-vis SEC experiments. Experiments were performed in DMF containing no alcohol (black trace), 1M ethylene glycol (orange trace), 2M ethanol (blue trace), or 2M tert-butanol (red trace) with 0.2 M $TBAPF_6$ electrolyte and 0.7 mM TCQ under CO_2 atmosphere. In the presence of 1M ethylene glycol, some protonation (to form the corresponding hydroquinone $TCQH_2$, green trace) is observed.

indistinguishable from those when CO_2 is added to an ethanol-containing solution of $[TBA]_2[TCQ^{2-}]$, which verifies that the same product is formed and establishes that CO_2 can insert into the hydrogen-bonds formed between ethanol and TCQ^{2-} in solution.

Once formed, $TCQ(CO_2)^{2-}$ can be oxidized, resulting in the loss of bound CO_2. UV-vis SEC with solutions of $[TBA]_2[TCQ^{2-}]$ in pure DMF or 2M EtOH in DMF show quantitative conversion into $TCQ^{\bullet-}$ or TCQ upon one or two-electron oxidation under both N_2 and CO_2 atmospheres (Figure S19 and SI for experimental details). These features are also present in the CVs of chemically synthesized $[TBA]_2[TCQ^{2-}]$ recorded in the presence or absence of EtOH under N_2 (Figure S8) or CO_2 atmosphere, when the species is $TCQ(CO_2)^{2-}$(Figure S18).

The anodic shift of $E(TCQ^{\bullet-}/ TCQ^{2-})_{1/2}$ under CO_2 versus N_2 atmosphere can be used to calculate the CO_2 binding constant ($K_{1,CO2}$) of TCQ^{2-} using equation 1 (see additional Equation 1 discussion in the SI).[31]

$$E_{1/2} = E^{o\prime} + \frac{RT}{nF}\ln\left(K_{CO_2}\right) + q\frac{RT}{nF}\ln\left[CO_2\right] \qquad \mathbf{1}$$

In equation 1, R is the gas constant, T is temperature, F is Faraday's constant, and n is the number of electrons being passed in the redox event (n = 1 for $E(TCQ^{\bullet-}/ TCQ^{2-})_{1/2}$). The number of CO_2 molecules that are bound is represented by the term q (which was previously determined to be one for TCQ).[12] $E^{\circ\prime}$ and $E_{1/2}$ are the half-wave potential in the absence of CO_2 and in the presence of a known CO_2 concentration in solution ($[CO_2]$), respectively. Using this method, the $\log(K_{CO2})$ of TCQ^{2-} is 3.7 ± 0.2 in the absence of hydrogen-bond donors in DMF.[12]

Comparison of the $E(TCQ^{\bullet-}/ TCQ^{2-})_{1/2}$ under N_2 and CO_2 atmospheres with alcohol additives were used to measure K_{CO2} according to equation 1. K_{CO2} steadily decreases (decreasing ΔE) with increasing concentrations of 5 of the 8 alcohols investigated (trifluoroethanol, tribromoethanol, ethylene glycol, 2-propanol, or *tert*-butanol) in both DMF and DMSO (Figure S20, S21). Thus, even though these alcohols shift $E^{\circ\prime}(TCQ^{\bullet-}/ TCQ^{2-})$ into the desired aerobic operating regime (green region, Figure 1), $K_{1,CO2}$ also decreases. As a result, these alcohols do not perform better than other functionalized quinones without hydrogen-bonding (Figure 1) for flue gas capture applications. However, three of the alcohols (ethanol, hexanol, and 2-methoxyethanol) exhibit the *opposite* behavior, with *increased* values of K_{CO2} at higher alcohol concentration (Figure S22). The increased CO_2 binding affinities at milder potentials afforded by these additives shifts TCQ into the desired operating regime for flue gas capture (black square vs. orange star, Figure 1), successfully breaking the LFER to make them viable candidates for eCCC from flue gas concentrations containing O_2.

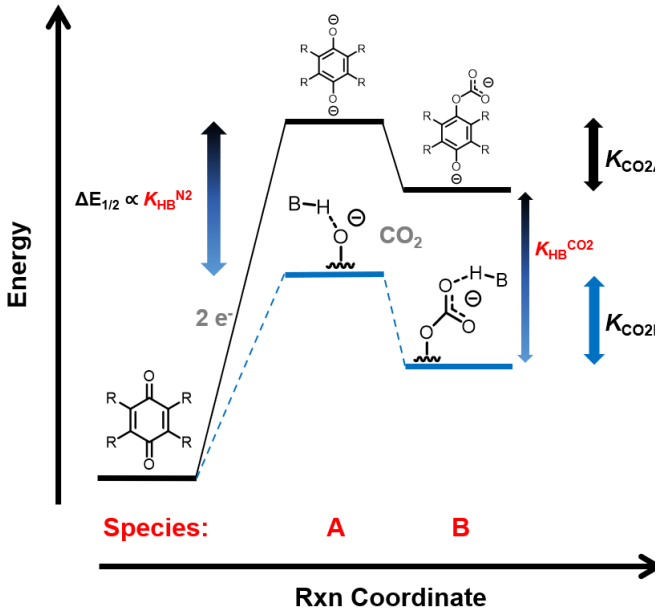

Figure 4. General reaction coordinate diagram of the two-electron reduction of a quinone and binding to CO_2 in the absence (black) or presence (blue) of a hydrogen-bonding donor.

Spectrophotometric experiments were used to independently verify the electrochemically-derived K_{CO2} values. Titration of $[TBA]_2[TCQ^{2-}]$ with CO_2 was monitored using electronic absorption

spectroscopy. $[TBA]_2[TCQ^{2-}]$ quantitatively converts into $TCQ(CO_2)^{2-}$ upon addition of 1 equivalent of CO_2 in pure DMF and 2M ethanol in DMF solutions (Figure S23). For each of the titrations, K_{CO2} was calculated from the disappearance of the absorption corresponding to TCQ^{2-} using the Benesi-Hildebrand method (Figure S23).[32,33] From this data, TCQ^{2-} has values of $\log(K_{CO2}) = 2.97 \pm 0.04$ and 3.4 ± 0.2 in pure DMF and 2M ethanol in DMF, respectively. While these values are slightly lower than those measured using voltametric methods ($\log(K_{CO2}) = 3.7 \pm 0.2$ and 4.3 ± 0.2 for DMF and 2M ethanol in DMF, respectively) they confirm the trend found using electrochemical methods. Importantly, the CO_2 binding constant measured by both methods in the presence of ethanol is sufficient for capture from flue gas concentrations.

Optimizing the Hydrogen-bonding Interactions with Reduced TCQ Species

In order to advance the development of air-stable eCCC carriers, it is important to understand why addition of ethanol, hexanol, and 2-methoxyethanol break the LFER for TCQ, while the other alcohols (trifluoroethanol, tribromoethanol, ethylene glycol, 2-propanol, and tert-butanol) do not. Figure 4 shows a general reaction coordinate diagram for quinone reduction and binding to one molecule of carbon dioxide based on an EEC mechanism.[12,13] Species A is the doubly reduced quinone dianion and species B is its CO_2 adduct. The interaction of a hydrogen-bond donor lowers the energy of both species A and B. The magnitude in which the two key redox carrier properties ($E_{1/2}$ and $K_{1,CO2}$) change relies on the relative energy changes of A and B. If the energies of species A and B are reduced by the same degree, there should be little to no effect on K_{CO2}, as it is directly dictated by the energy difference between the two species, however the reduction potential will be anodically shifted. As a result, proper tuning of intermolecular hydrogen-bonding interactions with both species A and B is required to break the LFER shown in Figure 1 and permit stability under aerobic conditions.

We hypothesized that the drop in K_{CO2} with increasing alcohol concentration for trifluoroethanol, tribromoethanol, ethylene glycol, 2-propanol, and tert-butanol was due to disproportionate stabilization of TCQ^{2-} versus $[TCQ(CO_2)]^{2-}$ (species A vs B in Figure 4). To evaluate this hypothesis, the strength of the hydrogen-bonding interactions between TCQ^{2-} and $[TCQ(CO_2)]^{2-}$ with each alcohol were quantified using cyclic voltammetry. The reduction of $TCQ^{\bullet-}$ to TCQ^{2-}, and consequent hydrogen-bond formation with n number of hydrogen-bond donors (HB), can be represented by the following chemical steps:

$$TCQ^{\bullet-} + e^- \rightleftharpoons TCQ^{2-}$$
$$TCQ^{2-} + n\,HB \rightleftharpoons TCQ^{2-}(HB)_n$$

From this series of equilibria and the Nernst equation, the equilibrium constant of the dianion with n molecules of hydrogen-bond donor, HB ($K_{HB}^{(2-)}$), can be calculated using equation 2[27] (more detail on equation 2 can be found in the SI).

$$\exp\left(f\Delta E(TCQ^{-1}/TCQ^{-2})_{1/2}\right) = 1 + K_{HB}^{(2-)}[HB]^n \qquad \mathbf{2}$$

The difference between K_{HB}^{CO2} and K_{HB}^{N2}, represented as $\Delta\mathrm{Log}(K_{HB}^{(2-)})$ (where $\Delta\mathrm{Log}(K_{HB}^{(2-)}) = K_{HB}^{N2} - K_{HB}^{CO2}$), effectively measures how much more (or less) the energy of TCQ^{2-} is lowered by hydrogen-bonding interactions compared to $[TCQ(CO_2)]^{2-}$ (displayed graphically in the reaction coordinate diagram shown in Figure 4). If a hydrogen-bond donor lowers the energy of $[TCQ(CO_2)]^{2-}$ more than TCQ^{2-} ($\Delta K_{HB}^{(2-)} < 0$), CO_2 binding will be more favorable and K_{CO2} will increase as the concentration of hydrogen-bond donor in solution

increases. Conversely, if the interaction with TCQ^{2-} is too strong($\Delta Log(K_{HB}^{(2-)}) > 0$), then CO_2 binding will be less favored, and K_{CO2} will decrease.

Table 1 lists values for $K_{HB}^{(2-)}$ and n under N_2 (K_{HB}^{N2}) or CO_2 (K_{HB}^{CO2}) atmosphere, as well as $\Delta Log(K_{HB}^{(2-)})$ for each of the alcohols investigated (plots used in the determination of each K_{HB} value are shown in Figures S24-S27). As shown in Figure 5A, there is a linear correlation between $log(K_{HB}^{N2})$and the pK_a[34–37] of the alcohol additive, where more acidic alcohols have larger values of K_{HB}^{N2}. Likewise, a plot of $log(K_{HB}^{CO2})$ versus pK_a[34–37] shows a similar linear relationship, albeit with a shallower slope (Figure 5B). The relationship between $\Delta Log(K_{HB}^{(2-)})$ and pK_a is not linear, but is in fact v-shaped (Figure 5C). $\Delta Log(K_{HB}^{(2-)})$ decreases with increasing pK_a up until a certain point ($pK_a \sim 16$), after which $\Delta Log(K_{HB}^{(2-)})$ starts increasing. Three of the alcohols investigated (ethanol, hexanol, and 2-methoxyethanol) have $\Delta Log(K_{HB}^{(2-)})$ values less than zero. This result is consistent with changes in K_{CO2} with increasing concentration of each of the alcohols investigated. Verifying our hypothesis, the correlation between $\Delta Log(K_{HB}^{(2-)})$ and K_{CO2} indicates that the hydrogen-bonding interactions of each alcohol with $[TCQ(CO_2)]^{2-}$ and TCQ^{2-} needs to be finely tuned to promote CO_2 binding at milder potentials. Thus, the alcohols with $\Delta Log(K_{HB}^{(2-)}) < 0$ have pK_a's around 16, while alcohols with either higher or lower pK_a have $\Delta Log(K_{HB}^{(2-)}) > 0$, although it is possible that the higher values of $\Delta Log(K_{HB}^{(2-)})$ for 2-propanol and *tert*-butanol are not a result of pK_a, but increased steric hindrance.

Table 1. Equilibrium constants for TCQ^{2-} and $TCQ(CO_2)^{2-}$ in DMF and DMSO under CO_2 and N_2 atmosphere with various alcohol hydrogen-bond donors.

	pK_a (H_2O)[†]	$Log(K_{HB}^{N2})$ (n)		$Log(K_{HB}^{CO2})$ (n)		$\Delta Log(K_{HB}^{(2-)})$		$Log(K_{CO2})$ ($\Delta E_{1/2}$ ~250 mV)	
***tert*-butanol (t-BuOH)**	**18.0**	1.1 (1.8)		0.51 (1.0)		0.57		(<< 2.4)*	
2-propanol (i-PrOH)	**17.0**	2.2 (2.2)		1.9 (1.8)		0.29		(<3.7)*	
Hexanol (HexOH)	**16.1**	2.6 (2.3)		3.2 (3.0)		–0.58		(>4.5)*	
Ethanol (EtOH)	**15.9**	3.4 (2.3)		4.0 (2.5)		–0.63		4.4	
2-methoxyethanol (2-ME)	**15.7**	2.4 (2.3)		2.9 (2.7)		–0.53		(>4.1)*	
Ethylene Glycol (EG)	**14.2**	6.9 (2.5)	4.4[a] (2.4)	6.4 (2.6)	3.6[a] (2.4)	0.52	0.72[a]	3.3	3.3[a]
Tribromoethanol (TBE)	**13.4**	5.5 (2.3)		3.7 (1.8)		1.8		2.5	
Trifluoroethanol (TFE)	**12.5**	7.4 (3.2)	4.9[a] (2.2)	5.6 (2.6)	3.0[a] (1.5)	1.8	1.9[a]	2.4	2.0[a]

[†] pK_a values obtained from references 34–37.
* $\Delta E_{1/2}$[2] of 250 mV was not reached at $[ROH] \leq 3$ M.
[a] Determined from measurements taken in DMSO.

In addition to alcohol pK_a, solvent identity also affects K_{HB}^{N2} and K_{HB}^{CO2}. Measured values of $K_{HB}^{(2-)}$ in DMSO are several orders of magnitude lower than those obtained in DMF (TFE and ethylene glycol, Table 1). Lower values of $K_{HB}^{(2-)}$ in DMSO likely arise from its larger solvent

donor number compared to DMF.[38] This would result in stronger hydrogen-bonds formed between the alcohol and solvent molecules that are more difficult to disrupt to form hydrogen-bonding interactions with TCQ^{2-} or $[TCQ(CO_2)]^{2-}$. This hypothesis is further supported by prior studies, which report K_{HB}^{N2} values for TCQ^{2-} with ethanol and TFE that are significantly larger in acetonitrile and benzonitrile (which have lower donating abilities than DMF or DMSO)[38] than what we measured in DMF and DMSO.[27]

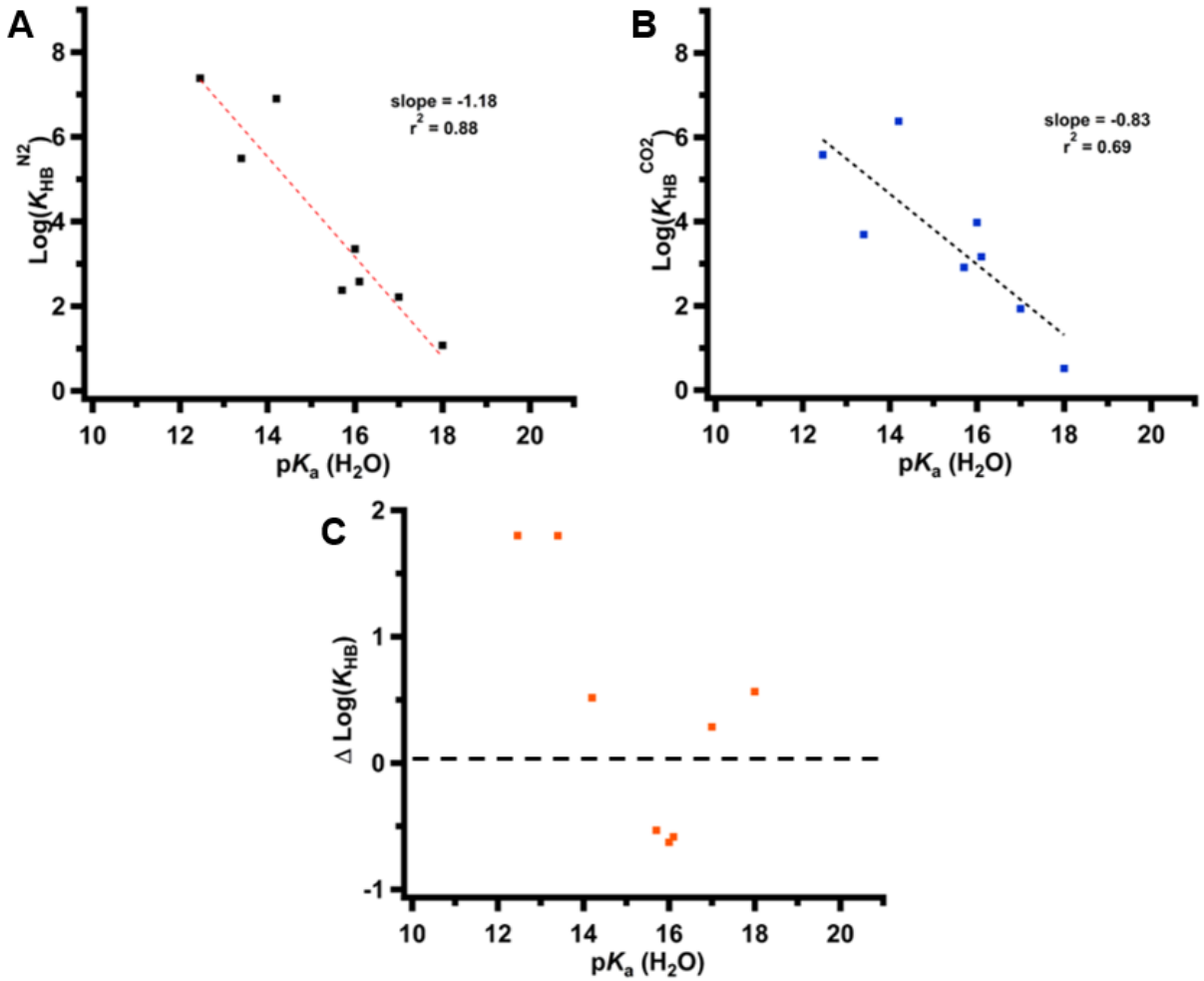

Figure 5. Hydrogen-bonding Interactions by Alcohol pK_a. Plots of Log(K_{HB}^{N2}) (A), Log(K_{HB}^{CO2}) (B), and ΔLog($K_{HB}^{(2-)}$) (C) versus alcohol pK_a (H_2O) for DMF solutions of TCQ containing various alcohol additives. The dotted black line indicates where ΔLog($K_{HB}^{(2-)}$) = 0.

From the alcohols studied, ethanol is the most promising candidate for use in an eCCC system utilizing TCQ as the redox carrier, due to its favorable values of K_{HB}^{CO2}, K_{HB}^{N2}, and ΔLog($K_{HB}^{(2-)}$). Ethanol's large K_{HB}^{N2} means that that $E(TCQ^{\bullet-}/TCQ^{2-})_{1/2}$ is shifted significantly positive without a large concentration of alcohol. For example, at 2M ethanol concentration, $E(TCQ^{\bullet-}/ TCQ^{2-})_{1/2}$ is shifted over 230 mV positive than in the absence of an alcohol (black traces, Figure 6). Importantly, this potential is 200 mV positive of $E(O_2/O_2^{\bullet-})_{1/2}$ (potential at half-maximum current = –1.30 V vs. $[Fe(C_5H_5)_2]^{+/0}$ at a glassy carbon electrode in pure DMF, or –1.20 V vs. $[Fe(C_5H_5)_2]^{+/0}$ in DMF containing 2M ethanol, Figure S1 and Figure 6 (below)), thereby avoiding undesirable losses in faradaic efficiency from O_2 reduction or carrier decomposition from

superoxide generation.[19,20] Additionally, K_{HB}^{CO2} is larger than K_{HB}^{N2} for ethanol, resulting in a negative $\Delta Log(K_{HB}^{(2-)})$ which indicates that CO_2 binding is not weakened by hydrogen-bonding interactions, but is in fact *strengthened* by them. Altogether, these properties indicate that when combined with a hydrogen-bond donor such as ethanol, TCQ becomes an effective redox carrier for eCCC from aerobic streams at flue gas concentrations.

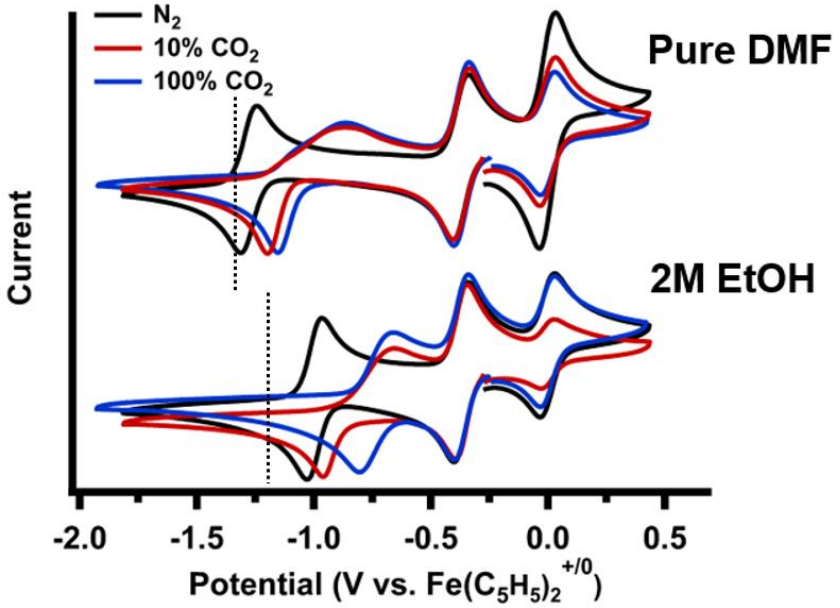

Figure 6. Cyclic voltammograms of TCQ in DMF and 2M EtOH in DMF under 1 atm N_2 and CO_2. Cyclic voltammograms of TCQ under N_2 (black), 10% CO_2 (red), or 100% CO_2 (blue) atmosphere in pure DMF (top) or 2M EtOH: DMF (bottom). Voltammograms were recorded at 100 mV/sec scan rate with solutions containing 0.2 M $TBAPF_6$ electrolyte and 2.0 mM TCQ. The reversible couple centered at 0.0 V corresponds to $[Fe(C_5H_5)_2]^{+/0}$. Vertical dotted black lines indicate the potential of $E(O_2/O_2^{\bullet-})_{1/2}$ in each solvent mixture (Figure S1).

Bulk CO_2 Capture and Release Studies

The combined redox and CO_2 binding properties of TCQ^{2-} with ethanol additives prompted us to investigate whether this system could be used to capture and release CO_2 from flue gas concentrations in the presence of O_2. A closed system was used to complete CO_2 capture and release from 10% CO_2 sources. The electrolysis was performed using a sealed H-cell similar to the one depicted in Figure 7A (and Figure S29), where the CO_2 concentration of the working cell headspace was periodically monitored through an IR CO_2 analyzer in a closed loop using a small pump that circulated the headspace. Each cycle was initiated by sparging a solution of chemically synthesized $[TBA]_2[TCQ^{2-}]$ in the working compartment with simulated flue gas to form $TCQ(CO_2)^{2-}$. An oxidizing potential was then applied to the working cell solution to release bound CO_2 and form $TCQ^{\bullet-}$. TCQ was used as a sacrificial oxidant in the counter cell to balance charge and limit undesirable crossover effects. Once oxidation was complete, the working cell solution was then reduced to reform TCQ^{2-} and capture the CO_2 released in the previous step.

In the absence of ethanol, CO_2 capture and release was tested with TCQ using simulated aerobic (87:10:3, N_2:CO_2:O_2 (v/v)) and anaerobic (90:10, N_2: CO_2 (v/v)) flue gas mixtures. Experimental details and results are described in the SI. Although capture and concentration are observed in both cases, decomposition occurs upon reduction of the carrier, which prevents re-capture of the CO_2 released.

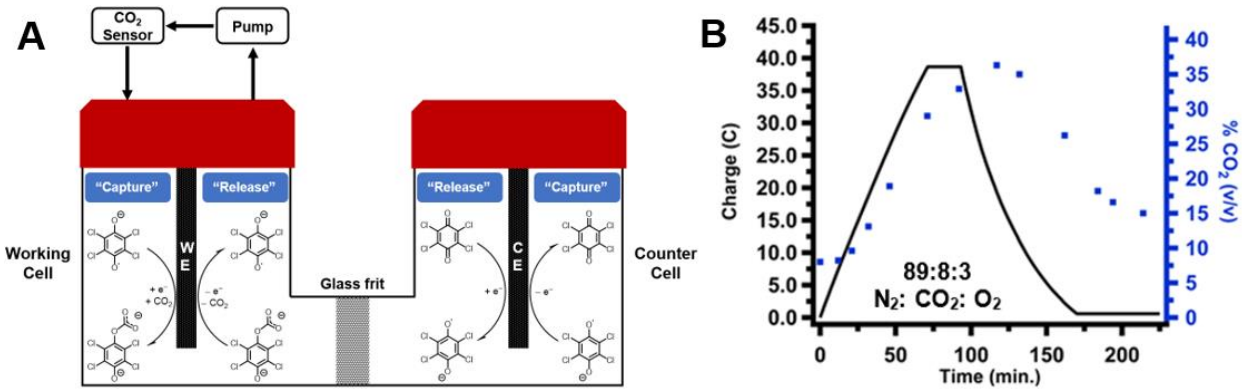

Figure 7. Electrochemical Cycle for CO_2 Capture and Release. A) Schematic of the H-cell setup utilized for electrochemical CO_2 capture electrolyses, showing the TCQ-based processes occurring in each cell during the capture and release steps of the eCCC cycle. B) Charge versus time plot (black trace) of electrochemical CO_2 capture and release from 89:8:3 N_2:CO_2:O_2 with $[TBA]_2[TCQ^{2-}]$ in 2M ethanol in DMF. Headspace CO_2 concentration was monitored periodically during the course of the experiment (blue squares).

When the same capture cycle experiment is performed in the presence of 2M ethanol, the system completes the entire electrochemical capture cycle. Under a 89:8:3, N_2:CO_2:O_2 (v/v) atmosphere, a 50 mM solution of $[TBA]_2[TCQ^{2-}]$ in 2M ethanol in DMF captured and concentrate CO_2 from 8.0% to 36.3% (v/v), passing 38.4 Coulombs of charge during the oxidation (Figure 7B). The initial and final headspace CO_2 concentration and charge passed corresponds to a 95% Faradaic efficiency (FE) and 98% yield of released CO_2 based on the moles of TCQ^{2-} in solution. The solution was then reduced once more until a total charge of –37.8 Coulombs was passed. The CO_2 concentration in the headspace decreased from 36.3% to 15% (v/v), resulting in a 73% FE for the re-capture step.

The use of ethanol as an additive to TCQ-based eCCC systems provides enhanced O_2 stability, which is essential for practical eCCC. The batch-capture experiments performed with a closed H-cell system is similar to a 3-stage capture system, where the redox carrier is reduced or "activated" in the presence of CO_2 before being pumped over to the anodic cell where it is oxidized to release bound CO_2.[3] The minimum thermodynamic requirement for this type of redox-carrier eCCC system can be estimated from the ΔE between the half-wave potentials of the carrier in the presence of its dilute CO_2 inlet stream (in this case, flue gas at 10% CO_2 v/v) and of its concentrated outlet stream (100% CO_2).[2,3,26,39] Cyclic voltammograms of TCQ in the presence and absence of 2M ethanol under 10 and 100% CO_2 are shown in Figure 6. In the absence of ethanol, ΔE of the half-wave potentials (conservatively measured as 30mV from the potential at peak current) under 10% CO_2 and 100% CO_2 (the conditions under capture and release during reduction and oxidation, respectively) is 250 mV. This ΔE value corresponds to a minimum calculated work of 23.3 kJ/mol CO_2 captured, or 24% energetic efficiency (based on a minimum theoretical requirement of 5.6 kJ/mol for a 10–100% CO_2 concentration swing). At 2M ethanol concentration, ΔE drops to 220 mV between 10 to 100% CO_2, lowering the calculated work required to just 21.5 kJ/mol, which raises the calculated maximum energetic efficiency to 26%, which is almost twice as efficient as any other reported eCCC method, or state-of-the-art alkanolamine-based systems.[21,23–26,40] We note that these calculations derive a minimum energetic requirement from the redox carrier

properties. In a full electrolytic system, other factors would contribute to the operating efficiency including cell overpotentials, carrier solubility, and CO_2 solubility, which could all be optimized through cell engineering. Additionally, the CO_2 binding constant of the redox carrier can be further optimized for specific CO_2 concentrations to achieve even higher efficiencies.

Conclusion

Electrochemical carbon dioxide capture and concentration (eCCC) can achieve significantly higher energy efficiencies than current thermal methods and its modular infrastructure is well-suited for mobile or point source applications. However, eCCC systems have been plagued by oxygen instability. This study describes the use of alcohol additives to modify the properties of a quinone CO_2 redox carrier through intermolecular hydrogen-bonding interactions. Optimizing these interactions through alcohol pK_a and concentration results in beneficial changes to the redox properties *and* CO_2 binding, the two key parameters of an eCCC redox carrier. With TCQ, the optimal interactions were achieved in 2M ethanol in DMF, with a maximum theoretical efficiency of 26% for concentrating a 10% CO_2 stream to 100%. With this combination of commercially available compounds, we demonstrate successful completion of a full cycle of electrochemical CO_2 capture and release in the presence of O_2 from flue gas concentrations, making a significant advance towards practical eCCC. Because the ideal redox carrier parameters will ultimately depend on the concentration of CO_2 in the targeted capture stream, this approach can be further used to generate a library of commercially available quinones and alcohol combinations optimized for application-specific, cost-effective, and scalable eCCC solutions.

Acknowledgments: This research was supported by the Alfred P. Sloan Foundation (JMB, JYY). We thank Alessandra Zito (UCI), Dr. Daniel Bim (UCLA), Prof. Anastassia Alexandrova (UCLA), Lauren Clarke (MIT), Dr. McLain Leonard (MIT), and Prof. Fikile Brushett (MIT) for helpful discussions.

Author contributions:

Conceptualization: JMB, JYY
Methodology: JMB
Investigation: JMB
Funding acquisition: JYY
Project administration: JYY
Supervision: JYY
Writing – original draft: JMB
Writing – review & editing: JYY

Competing interests: Authors declare that they have no competing interests
Materials & Correspondence: j.yang@uci.edu
Data and materials availability: All data are available in the main text or the supplementary materials.

Supplementary Materials

Materials and Methods
Supplementary Text
Figs. S1 to S30

Tables S1 to S4
References (*1-15*)

References:

(1) Sanz-Pérez, E. S.; Murdock, C. R.; Didas, S. A.; Jones, C. W. Direct Capture of CO2 from Ambient Air. *Chem. Rev.* **2016**, *116* (19), 11840–11876. https://doi.org/10.1021/acs.chemrev.6b00173.

(2) Stern, M. C.; Simeon, F.; Hammer, T.; Landes, H.; Herzog, H. J.; Alan Hatton, T. Electrochemically Mediated Separation for Carbon Capture. *Energy Procedia* **2011**, *4*, 860–867. https://doi.org/https://doi.org/10.1016/j.egypro.2011.01.130.

(3) Shaw, R. A.; Hatton, T. A. Electrochemical CO2 Capture Thermodynamics. *Int. J. Greenh. Gas Control* **2020**, *95*, 102878. https://doi.org/https://doi.org/10.1016/j.ijggc.2019.102878.

(4) Rheinhardt, J. H.; Singh, P.; Tarakeshwar, P.; Buttry, D. A. Electrochemical Capture and Release of Carbon Dioxide. *ACS Energy Lett.* **2017**, *2* (2), 454–461. https://doi.org/10.1021/acsenergylett.6b00608.

(5) Renfrew, S. E.; Starr, D. E.; Strasser, P. Electrochemical Approaches toward CO2 Capture and Concentration. *ACS Catal.* **2020**, *10* (21), 13058–13074. https://doi.org/10.1021/acscatal.0c03639.

(6) Sharifian, R.; Wagterveld, R. M.; Digdaya, I. A.; Xiang, C.; Vermaas, D. A. Electrochemical Carbon Dioxide Capture to Close the Carbon Cycle. *Energy Environ. Sci.* **2021**, *14* (2), 781–814. https://doi.org/10.1039/D0EE03382K.

(7) Ranjan, R.; Olson, J.; Singh, P.; Lorance, E. D.; Buttry, D. A.; Gould, I. R. Reversible Electrochemical Trapping of Carbon Dioxide Using 4,4′-Bipyridine That Does Not Require Thermal Activation. *J. Phys. Chem. Lett.* **2015**, *6* (24), 4943–4946. https://doi.org/10.1021/acs.jpclett.5b02220.

(8) Singh, P.; Tarakeshwar, P.; Buttry, D. A. Experimental, Simulation, and Computational Study of the Interaction of Reduced Forms of N-Methyl-4,4'-Bipyridinium with CO2. *ChemElectroChem* **2020**, *7* (2), 469–475. https://doi.org/https://doi.org/10.1002/celc.201901884.

(9) Ishida, H.; Ohba, T.; Yamaguchi, T.; Ohkubo, K. Interaction between CO₂ and Electrochemically Reduced Species of N-Propyl-4,4′-Bipyridinium Cation. *Chem. Lett.* **1994**, *23* (5), 905–908. https://doi.org/10.1246/cl.1994.905.

(10) Singh, P.; Rheinhardt, J. H.; Olson, J. Z.; Tarakeshwar, P.; Mujica, V.; Buttry, D. A. Electrochemical Capture and Release of Carbon Dioxide Using a Disulfide–Thiocarbonate Redox Cycle. *J. Am. Chem. Soc.* **2017**, *139* (3), 1033–1036. https://doi.org/10.1021/jacs.6b10806.

(11) Bell, W. L.; Miedaner, A.; Smart, J. C.; DuBois, D. L.; Verostko, C. E. Synthesis and Evaluation of Electroactive CO_2 Carriers. *SAE Trans.* **1988**, *97*, 544–552.

(12) DuBois, D. L.; Miedaner, A.; Bell, W.; Smart, J. C. Chapter 4 - ELECTROCHEMICAL CONCENTRATION OF CARBON DIOXIDE. In *Electrochemical and Electrocatalytic Reactions of Carbon Dioxide*; Sullivan, B. P., Ed.; Elsevier: Amsterdam, 1993; pp 94–117.

https://doi.org/https://doi.org/10.1016/B978-0-444-88316-2.50008-5.

(13) Nagaoka, T.; Nishii, N.; Fujii, K.; Ogura, K. Mechanisms of Reductive Addition of CO2 to Quinones in Acetonitrile. *J. Electroanal. Chem.* **1992**, *322* (1), 383–389. https://doi.org/https://doi.org/10.1016/0022-0728(92)80090-Q.

(14) De Sousa Bulhõesw, L. O.; Zara, A. J. The Effect of Carbon Dioxide on the Electroreduction of 1,4-Benzoquinone. *J. Electroanal. Chem. Interfacial Electrochem.* **1988**, *248* (1), 159–165. https://doi.org/https://doi.org/10.1016/0022-0728(88)85158-1.

(15) Qiao, X.; Li, D.; Cheng, L.; Jin, B. Mechanism of Electrochemical Capture of CO2 via Redox Cycle of Chlorinated 1,4-Naphthoquinone in BMIMBF4: An in-Situ FT-IR Spectroelectrochemical Approach. *J. Electroanal. Chem.* **2019**, *845*, 126–136. https://doi.org/https://doi.org/10.1016/j.jelechem.2019.05.057.

(16) Namazian, M.; Zare, H. R.; Yousofian-Varzaneh, H. Electrochemical Behavior of Tetrafluoro-p-Benzoquinone at the Presence of Carbon Dioxide: Experimental and Theoretical Studies. *Electrochim. Acta* **2016**, *196*, 692–698. https://doi.org/https://doi.org/10.1016/j.electacta.2016.02.159.

(17) Comeau Simpson, T.; Durand, R. R. Reactivity of Carbon Dioxide with Quinones. *Electrochim. Acta* **1990**, *35* (9), 1399–1403. https://doi.org/https://doi.org/10.1016/0013-4686(90)85012-C.

(18) Mizen, M. B.; Wrighton, M. S. Reductive Addition of CO 2 to 9,10-Phenanthrenequinone. *J. Electrochem. Soc.* **1989**, *136* (4), 941–946. https://doi.org/10.1149/1.2096891.

(19) Boujlel, K.; Simonet, J. On the Electrochemical Reduction of α-Diketones in the Presence of Oxygen. *Tetrahedron Lett.* **1979**, *20* (12), 1063–1066. https://doi.org/https://doi.org/10.1016/S0040-4039(01)87192-6.

(20) Jeziorek, D.; Ossowski, T.; Liwo, A.; Dyl, D.; Nowacka, M.; Woźnicki, W. Theoretical and Electrochemical Study of the Mechanism of Anthraquinone-Mediated One-Electron Reduction of Oxygen: The Involvement of Adducts of Dioxygen Species to Anthraquinones. *J. Chem. Soc. Perkin Trans. 2* **1997**, No. 2, 229–236. https://doi.org/10.1039/A605549D.

(21) Scovazzo, P.; Poshusta, J.; DuBois, D.; Koval, C.; Noble, R. Electrochemical Separation and Concentration of <1% Carbon Dioxide from Nitrogen. *J. Electrochem. Soc.* **2003**, *150* (5), D91. https://doi.org/10.1149/1.1566962.

(22) *The Exact Number Depends on the Solvent-Dependent Henry's Constant for CO2. For Flue Gas (10% CO2), Log(KCO2) Must Be Greater than: 3.0 (DMF), 3.2 (DMSO), or 2.9 (CH3CN). For Atmospheric Concentration, Log(KCO2) Must Be Greater than: 5.5 (DMF, DMSO) or 5* .

(23) Voskian, S.; Hatton, T. A. Faradaic Electro-Swing Reactive Adsorption for CO2 Capture. *Energy Environ. Sci.* **2019**, *12* (12), 3530–3547. https://doi.org/10.1039/C9EE02412C.

(24) Rochelle, G.; Chen, E.; Freeman, S.; Van Wagener, D.; Xu, Q.; Voice, A. Aqueous Piperazine as the New Standard for CO2 Capture Technology. *Chem. Eng. J.* **2011**, *171* (3), 725–733. https://doi.org/https://doi.org/10.1016/j.cej.2011.02.011.

(25) Boot-Handford, M. E.; Abanades, J. C.; Anthony, E. J.; Blunt, M. J.; Brandani, S.; Mac

Dowell, N.; Fernández, J. R.; Ferrari, M.-C.; Gross, R.; Hallett, J. P.; Haszeldine, R. S.; Heptonstall, P.; Lyngfelt, A.; Makuch, Z.; Mangano, E.; Porter, R. T. J.; Pourkashanian, M.; Rochelle, G. T.; Shah, N.; Yao, J. G.; Fennell, P. S. Carbon Capture and Storage Update. *Energy Environ. Sci.* **2014**, *7* (1), 130–189. https://doi.org/10.1039/C3EE42350F.

(26) Liu, Y.; Ye, H.-Z.; Diederichsen, K. M.; Van Voorhis, T.; Hatton, T. A. Electrochemically Mediated Carbon Dioxide Separation with Quinone Chemistry in Salt-Concentrated Aqueous Media. *Nat. Commun.* **2020**, *11* (1), 2278. https://doi.org/10.1038/s41467-020-16150-7.

(27) Gupta, N.; Linschitz, H. Hydrogen-Bonding and Protonation Effects in Electrochemistry of Quinones in Aprotic Solvents. *J. Am. Chem. Soc.* **1997**, *119* (27), 6384–6391. https://doi.org/10.1021/ja970028j.

(28) Zhu, X.-Q.; Wang, C.-H.; Liang, H. Scales of Oxidation Potentials, PKa, and BDE of Various Hydroquinones and Catechols in DMSO. *J. Org. Chem.* **2010**, *75* (21), 7240–7257. https://doi.org/10.1021/jo101455m.

(29) Zanello, P. *Inorganic Electrochemistry: Theory, Practice and Application*; The Royal Society of Chemistry: Cambridge, UK, 2003.

(30) Bard, A. J.; Faulkner, L. R. *Electrochemical Methods: Fundamentals and Application*, 2nd ed.; Swain, E., Ed.; John Wiley & Sons, Inc.: Hoboken, NJ, 2001.

(31) Schmidt, M. H.; Miskelly, G. M.; Lewis, N. S. Effects of Redox Potential, Steric Configuration, Solvent, and Alkali Metal Cations on the Binding of Carbon Dioxide to Cobalt(I) and Nickel(I) Macrocycles. *J. Am. Chem. Soc.* **1990**, *112* (9), 3420–3426. https://doi.org/10.1021/ja00165a027.

(32) Benesi, H. A.; Hildebrand, J. H. A Spectrophotometric Investigation of the Interaction of Iodine with Aromatic Hydrocarbons. *J. Am. Chem. Soc.* **1949**, *71* (8), 2703–2707. https://doi.org/10.1021/ja01176a030.

(33) Kuntz, I. D.; Gasparro, F. P.; Johnston, M. D.; Taylor, R. P. Molecular Interactions and the Benesi-Hildebrand Equation. *J. Am. Chem. Soc.* **1968**, *90* (18), 4778–4781. https://doi.org/10.1021/ja01020a004.

(34) Chemistry., I. U. of P. and A.; Data., C. on E.; Serjeant, E. P.; Dempsey, B.; Chemistry., I. U. of P. and A.; Data., C. on E. *Ionisation Constants of Organic Acids in Aqueous Solution*; Pergamon Press: Oxford; New York, 1979.

(35) Reeve, W.; Erikson, C. M.; Aluotto, P. F. A New Method for the Determination of the Relative Acidities of Alcohols in Alcoholic Solutions. The Nucleophilicities and Competitive Reactivities of Alkoxides and Phenoxides. *Can. J. Chem.* **1979**, *57* (20), 2747–2754. https://doi.org/10.1139/v79-444.

(36) Takahashi, S.; Cohen, L. A.; Miller, H. K.; Peake, E. G. Calculation of the PKa Values of Alcohols from .Sigma. Constants and from the Carbonyl Frequencies of Their Esters. *J. Org. Chem.* **1971**, *36* (9), 1205–1209. https://doi.org/10.1021/jo00808a010.

(37) Ballinger, P.; Long, F. A. Acid Ionization Constants of Alcohols. I. Trifluoroethanol in the Solvents H2O and D2O1. *J. Am. Chem. Soc.* **1959**, *81* (5), 1050–1053. https://doi.org/10.1021/ja01514a010.

(38) Gutmann, V. Solvent Effects on the Reactivities of Organometallic Compounds. *Coord. Chem. Rev.* **1976**, *18* (2), 225–255. https://doi.org/https://doi.org/10.1016/S0010-8545(00)82045-7.

(39) Clarke, L. E.; Leonard, M. E.; Hatton, T. A.; Brushett, F. R. Thermodynamic Modeling of CO2 Separation Systems with Soluble, Redox-Active Capture Species. *ChemRxiv* **2021**. https://doi.org/10.33774/chemrxiv-2021-2dqk6.

(40) Rochelle, G. T. Amine Scrubbing for CO_2 Capture. *Science (80-.).* **2009**, *325* (5948), 1652–1654. https://doi.org/10.1126/science.1176731.